

The Influence of Load History on Synthetic Rope Response

S. Weller*, P. Davies†, L. Johanning*

*CEMPS Renewable Energy, University of Exeter, United Kingdom

E-mail: S.Weller@exeter.ac.uk, L.Johanning@exeter.ac.uk

†IFREMER, 29280 Plouzane, France

E-mail: Peter.Davies@ifremer.fr

Abstract—Although used for the station-keeping of offshore equipment for several decades, synthetic ropes have only recently been used for marine renewable energy (MRE) devices. The fundamental mooring load differences between these two applications necessitate the detailed quantification of mooring component performance. Of particular importance for lifecycle analysis, installation and maintenance operations is the evolution of synthetic component performance over time due to load history and fatigue mechanisms. Changes to the stiffness and damping properties of these materials will affect the global response of the device if the mooring system and device responses are closely coupled. To address these uncertainties, tension experiments have been conducted on Nylon parallel-stranded rope samples at IFREMER as part of a MERiFIC (Marine Energy in Far Peripheral and Island Communities) consortium. Measurements are reported from tests involving three new samples subjected to a mixed creep/recovery and harmonic loading regime. Different initial bedding-in levels are used to investigate the influence of load history on the immediate quasi-static and dynamic properties of the rope. For the load regimes studied, it is found that the rope condition with respect to the load-strain characteristic has a strong influence on the performance of the line.

Index Terms—Synthetic rope, axial stiffness, hysteresis, damping, load history, dynamic and quasi-static loads

I. INTRODUCTION

Considerable time and effort has been devoted to the testing and certification of synthetic mooring ropes over the past two decades by the oil and gas industry, due to apparent advantages in terms of cost, ease of handling and the ability to reduce peak loadings compared to steel components. This has led to the development of guidelines and standards including those produced by Bureau Veritas, the International Standards Organisation, Det Norske Veritas (DNV) and American Bureau of Shipping [1]–[4]. It is likely that synthetic ropes, for similar cost and performance reasons, will feature in the mooring systems of marine renewable energy (MRE) devices [5] and recommendations have been produced to pre-empt the shift from conventional chain moorings (The Carbon Trust/DNV [6]). These guidelines mainly refer to mooring for large offshore equipment, and their applicability is questionable for small, responsive devices such as wave energy converters (WECs), due to differences in water depth, load regimes, mass distribution, mooring system footprint and expected environmental conditions.

Numerical and experimental models have demonstrated the need to account for non-linear mooring line properties in fully dynamic MRE device models to accurately predict the performance of these devices as well as the associated fatigue life and capacity to withstand extreme loads of mooring components [7]. For dynamically responsive equipment such capabilities will be significantly influenced by the mechanical properties of mooring components (primarily axial stiffness and damping) [8], [9] as well as other loading mechanisms (i.e. viscous drag and added mass). Although particular properties (i.e. ultimate strength and axial stiffness) have been quantified in previous rope studies (e.g. [10]–[13]), the loading regimes used and rope constructions tested have been biased for large, slow-moving equipment used in the oil and gas industry (e.g. exploration and distribution platforms) and often material and structural damping have not been reported. To address this knowledge gap, the axial stiffness and damping of several Nylon 6 rope samples are quantified in this study in the context of rapidly changing mooring loads experienced by MRE devices. Insight gained through the dedicated component testing program [14], [15], will enable the design of economical mooring systems and facilitate the development of guidelines and standards which are more relevant to MRE devices (e.g. IEC-TS 62600-10 Ed.1.0 [16]).

In the next section the experimental equipment used in this study is outlined. The loading regimes applied to the rope samples are then defined in context of measurements recorded by the South West Mooring Test Facility (SWMTF). The experimental method and analysis techniques applied are then summarised. In Section 3 results are presented from harmonic load tests involving three new rope samples subjected to different levels of initial ‘bedding-in.’

II. EXPERIMENTAL APPROACH

A. Equipment used

The synthetic rope studied has a parallel-stranded subrope construction comprising multi-filament Nylon 6 fibres. Manufactured by Bridon International Ltd, the rope comprises seven subropes surrounded by a non-load bearing jacket, giving a cross-sectional diameter of 0.044m (Figure

1a). The minimum break load (MBL) as specified by the manufacturer is equal to 466kN. This rope is used in the upper 20m of the three catenary mooring lines used on the South West Mooring Test Facility (SWMTF; Figure 1b). Chains and a drag anchor are used for the lower sections of each mooring line, with the facility located in an average water depth of 30m in Falmouth Bay. On the surface is an instrumented buoy which includes a multi-axis inertial 'MotionPack' (20Hz sampling rate) and a digital GPS unit (10Hz sampling rate) as well as digital compass and sensors to measure temperature, wind velocity and salinity. For each mooring limb, tensions are simultaneously recorded by a three-axis load cell in addition to an axial load cell at a sample rate of 20Hz. Current velocities in the water column and surface elevations are recorded at 2Hz using a seabed-mounted 4-beam Acoustic Doppler Current Profiler (ADCP) located nearby. Only the tension measurements recorded by the axial load cells connecting the Nylon rope section to a swivel assembly mounted on the buoy are studied here. Further details regarding the system can be found in [17].

Three new rope samples were subjected to several loading regimes in dry conditions using the 100 Tonne hydraulic test machine at L'Institut Français de Recherche pour l'Exploitation de la Mer (IFREMER) in Brest, France. The IFREMER machine has the capability of testing samples up to 10m long in quasi-static and dynamic conditions, with a displacement amplitude of up to 0.75m (Figure 1c). Extension of the free length of the sample was measured over a distance of 1.1m using a pull-wire transducer clamped to the rope. For ropes without a protective jacket a video extensometry system developed at IFREMER can be used. The samples were supplied pre-spliced by the manufacturer with an eye-to-eye distance of approximately 5m.

B. Loading Regimes

The rope samples are subjected to load regimes based on mooring line tensions measured by the SWMTF between June 2009 and September 2011. Although the SWMTF does not have a power take-off system, the mooring loads recorded by the system are relevant to buoy-like MRE devices deployed in similar environmental conditions. In Figure 2a and b, examples of measured tension time-series as recorded by the axial load cells of the SWMTF in calm ($H_s \approx 0.86\text{m}$, $T_p \approx 5.1\text{s}$, 30.3-30.7m average water depth) and mild-storm ($H_s \approx 2.67\text{m}$, $T_p \approx 7.5\text{s}$, 31.9-32m average water depth) conditions are shown to illustrate the range of loads experienced by the mooring lines due to wave and tidal loading. In the plotted calm conditions, the average tension for Lines 1-3 is 3.77kN, corresponding to 0.8% of the rope MBL. These loads clearly contrast those measured during the mild-storm conditions, where an average tension of 5.97kN was recorded. In the plotted time-series the majority of loads are low amplitude

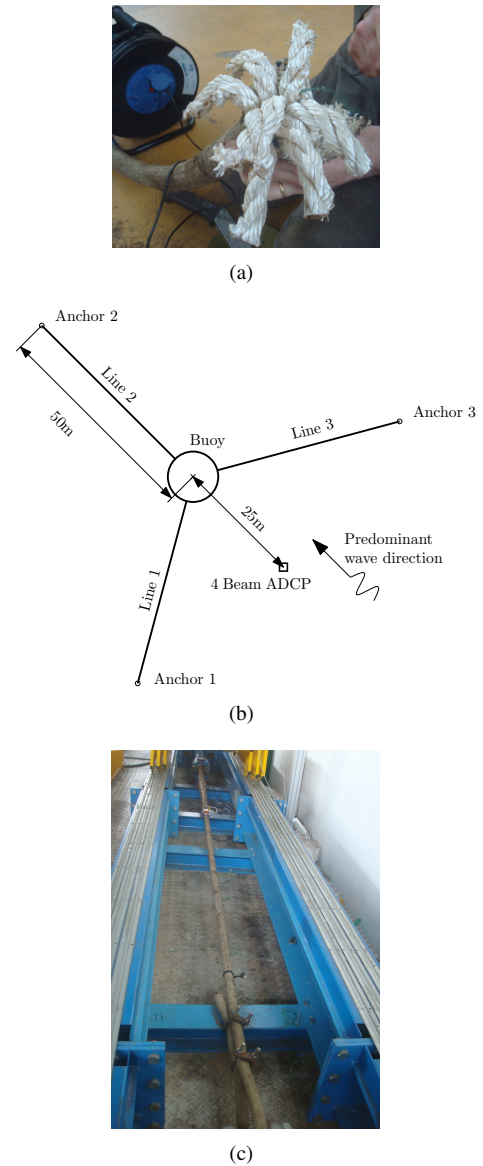
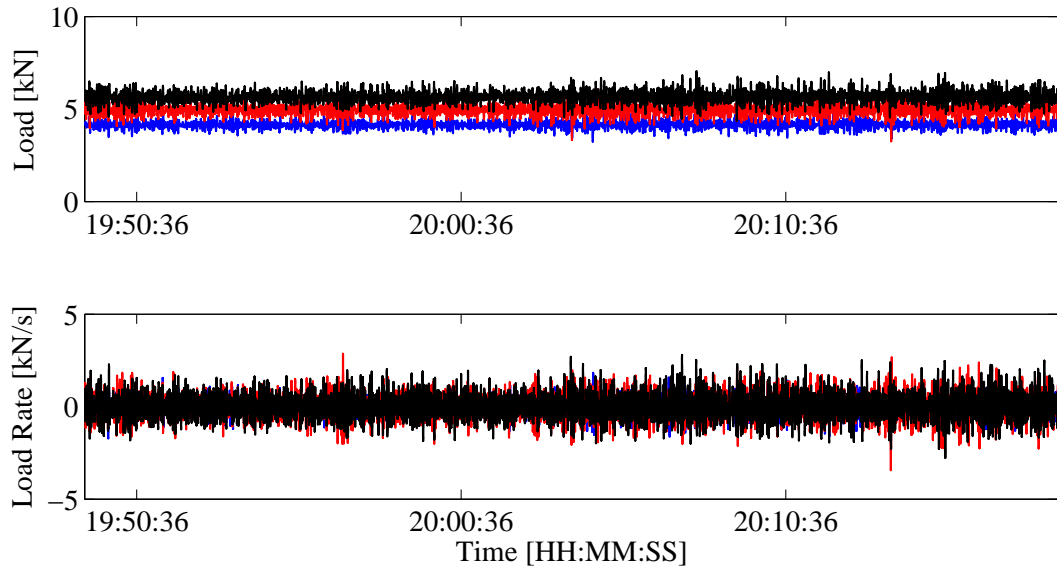
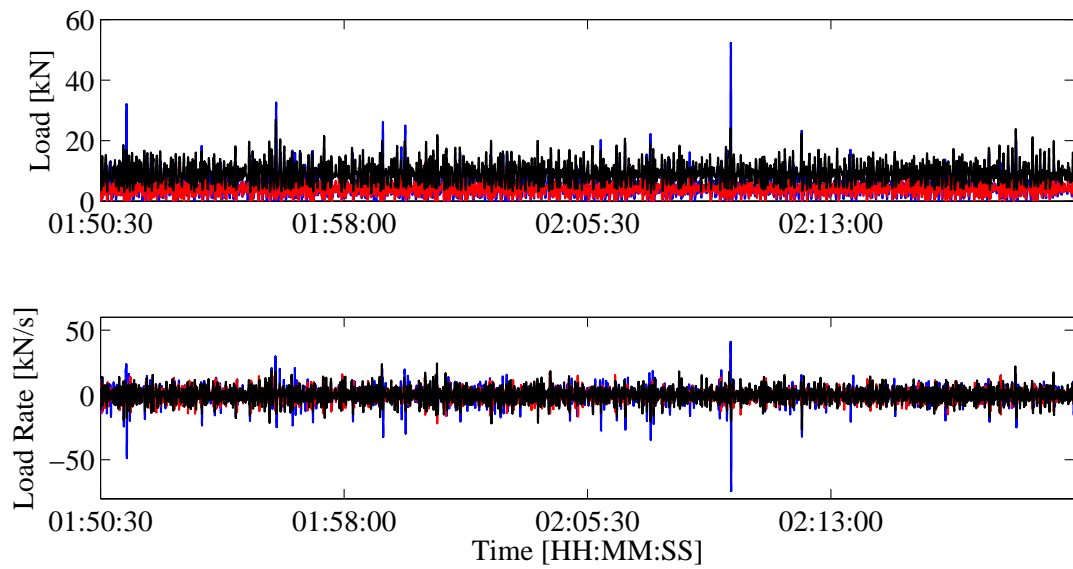


Fig. 1. a) Aged rope with outer jacket removed showing parallel-strand construction. b) SWMTF mooring arrangement and ADCP location (not to scale). c) IFREMER 100 Tonne machine used for rope testing

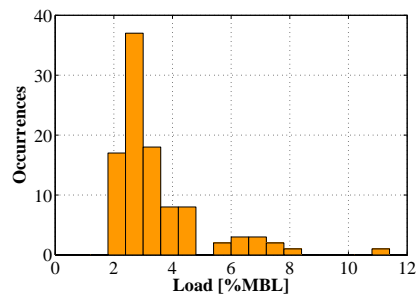
and in the range of 0-4% of the rope's MBL, in which the stiffness of the rope is highly non-linear [18]. A notable snatch load of 0-52.22kN (0-11.2% MBL) in the measured time-series occurs for Line 1 at 02:09:55. This short duration extreme load does not directly correspond with a large wave peak, but instead is due to the dynamic response of the buoy and mooring system, giving insight into the survivability of the system.



(a)



(b)



(c)

Fig. 2. Axial mooring tensions and calculated load rates for Line 1 (blue line), Line 2 (red line) and Line 3 (black line) measured during a) calm (28/09/2010-29/09/2010) and b) mild-storm (17/11/2010) conditions. c) Number of occurrences of significant loads identified from tension measurements for all three lines recorded during the first deployment [14].

Sample	Number of cycles	Minimum load	Maximum load	Ramp duration	Ramp load rate	Hold duration
1	None	N/A	N/A	N/A	N/A	N/A
2	10	2kN (0.4% MBL)	93.2kN (20% MBL)	150s	0.61kN/s	300s
3			186.4kN (40% MBL)		1.23kN/s	

TABLE I
BED-IN CYCLES USED ON SAMPLES 2 AND 3

Load level	Creep/recovery cycle				Harmonic intervals					
	Ramp load range	Ramp duration	Ramp load rate	Hold duration	Load range	Mean load	Ramp duration	Hold duration between intervals	Number of cycles	Oscillation periods and maximum load rates
A	2-23.3kN	30s	0.71kN/s	60s	2-23.3kN	12.7kN	30s	60s	25	50s (1.34kN/s), 25s (2.66kN/s), 100s (0.67kN/s)
B	2-46.6kN	60s	0.74kN/s		13.6-35.0kN	24.3kN				
C	2-69.9kN	90s	0.75kN/s		25.2-46.6kN	35.9kN				
D	2-93.2kN	120s	0.76kN/s		36.9-58.3kN	47.6kN				
E	2-116.5kN	150s	0.76kN/s		48.6-70.0kN	59.3kN				
	Steady load	Duration								
F	3.5kN	3600s								
G	2kN	38880s								

TABLE II
CREEP/RECOVERY, HARMONIC AND STEADY LOADING USED ON SAMPLES 1-3

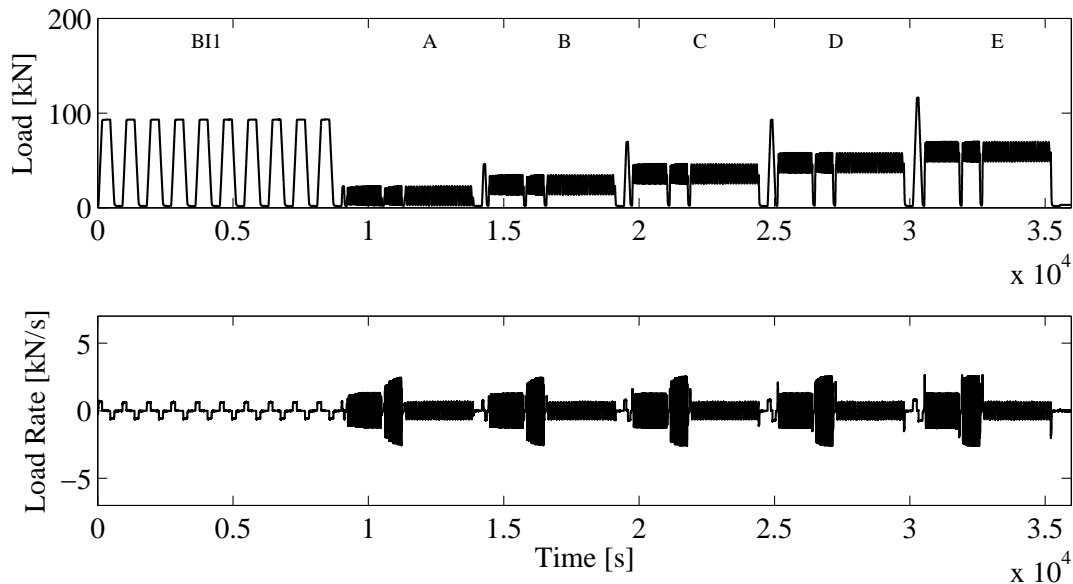


Fig. 3. Measured loads and load rate time-series' for the first 9.9 hours of the Sample 2 test

Analysis of the axial mooring loads measured during the first deployment indicate that a peak load of this magnitude was an isolated event, with most loads lower than 8% MBL (Figure 2c; details of the identification method used are outlined in [14]). The range of mooring tensions measured by the SWMTF imply that existing offshore component, operation and maintenance standards for larger, more slowly moving equipment (e.g. [3]) are not directly applicable to buoy-like MRE devices deployed in highly dynamic environments. For these applications there is considerable uncertainty about the operational and fatigue performance of these synthetic ropes over the lifetime of the system. To

contribute to the reduction of these uncertainties, tension testing equipment at IFREMER is utilised to ascertain the performance of this rope using relevant loading regimes. Of particular focus for this study is how the operational properties of the rope evolve with usage. Bedding-in cycles are applied to enable non-recoverable elongation of the rope from its manufactured state occurring due to macroscopic and molecular changes in the structure and fibres. Of the three new samples, Sample 1 is treated as a control specimen and no bedding-in cycles are applied, with Samples 2 and 3 subjected to ten cycles of bedding-in up to 20% and 40% of the MBL, as defined in Table I. All three samples are

then subjected to an initial creep/recovery cycle followed by harmonic loading at three different oscillation periods (50s, 25s and 100s). After a short hold of 300s at 2kN, this process is repeated for four more load levels up to a maximum load of 116.5kN (25% MBL), Table II. After the harmonic loading cycles, the load is maintained at 3.5kN for 1 hour and then for 10 hours at 2kN to determine the level of strain recovery and permanent sample extension. An example measured load and load rate time-series for Sample 2 is shown in Figure 3, showing similar load rates to those measured by the SWMTF during calm conditions (Figure 2a).

C. Measurement analysis procedure

Axial stiffness (EA) of the free rope length is calculated as the gradient of a single degree-of-freedom trend line fitted using the least squares method to measured load (F ; independent variable) and strain (ε ; dependent variable) values over each oscillation cycle. This approach contrasts the commonly used method in which the gradient between maximum and minimum load and strain values is used [19]. Comparisons between the two methods will feature in a forthcoming publication. Building upon the work carried out by Johannig et al. [8], damping which includes material and structural contributions, is calculated using the energy dissipated over each load-unload cycle (E_d), the angular frequency of the oscillation and the amplitude of piston displacement (X):

$$B = \frac{E_d}{\pi\omega X^2} \quad (1)$$

The start and end of each oscillation cycle are defined by the calculated strain and extension (e) minima, for axial stiffness and damping calculations respectively. Both quantities are then averaged over the last five oscillation cycles of each interval. For fully closed hysteresis loops the energy dissipated can be approximated by finding the area enclosed within each extension-force loop using trapezoidal integration (Figure 4a):

$$E_d = E_{load} - E_{unload} \quad (2)$$

When temporary or permanent extension of the sample occurs due to constructional rearrangement and/or material changes, hysteresis loops are typically open (Figure 4b) and in this case the integration is bounded by the cycle start, end and maximum measured elongations (e_1 , e_2 and e_{max}) as well as the start and end forces (F_{e1} and F_{e2}). The energy which is unrecovered at the end of the cycle (E_{unrec}) is estimated from the area under a single degree-of-freedom line fitted to the force and extension values at the beginning and end of each cycle. For the loading regimes specified in this study the estimated unrecovered energy tends to be significant for the creep/recovery cycles (e.g. $E_{unrec} = 0.06E_{load}$, for the example shown in Figure 4b). In this analysis it is therefore

assumed that the rope can be treated as a closed-system in which energy transferred out of the system (e.g. heat losses) is not taken into account.

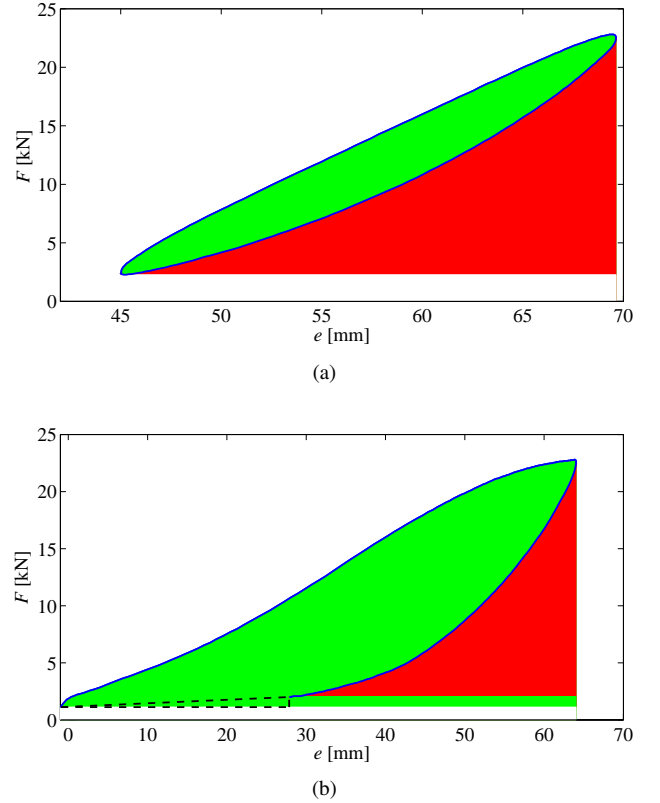


Fig. 4. Examples of a) closed and b) open hysteresis loops for Sample 1 showing energy during loading (E_{load} ; green region), energy during unloading (E_{unload} ; red region). In b) the first creep/recovery cycle is shown with apparent unrecovered energy (E_{unrec}) defined as the area bounded by the dashed line

III. INFLUENCE OF BEDDING-IN CYCLES ON NEW ROPE PERFORMANCE

A. Time-varying strain performance

In Figure 5a calculated time-varying strain values are presented for the three different samples. The strain values for Sample 1 have been aligned by the minimum force measurement of the first creep/recovery cycle (at $t = 9046s$). Here, strain is defined as the ratio of instantaneous extension to original length (measured before the start of each test with the sample pretensioned at 2kN). There is a distinct difference in the evolution of strain for the three samples. Comparing the response of the bedded-in samples (2 and 3), the highest strains can be attributed to Sample 3 which was subjected to the highest bedding-in level. Without bedding-in, the strain of Sample 1 is lower for the first three harmonic loading intervals and then highest for the last load level. Extension

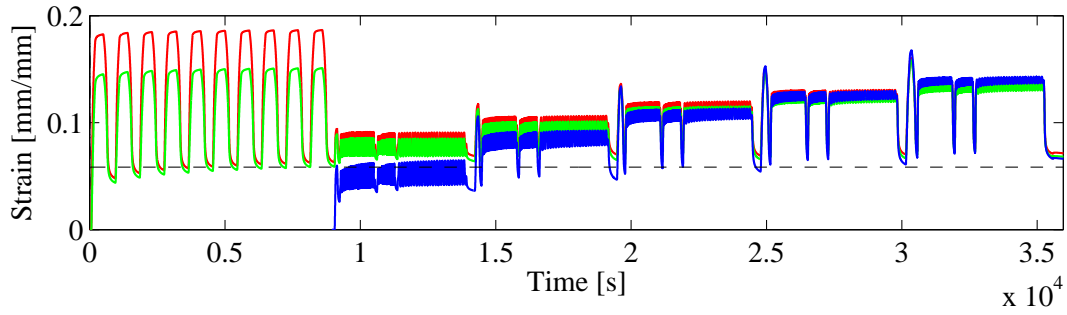


Fig. 5. Calculated time-varying strain values for Sample 1 (blue line), Sample 2 (green line) and Sample 3 (red line) during the first 9.9 hours of testing. The average strain of the three samples after 20.7 hours is shown as a black dash-dot line

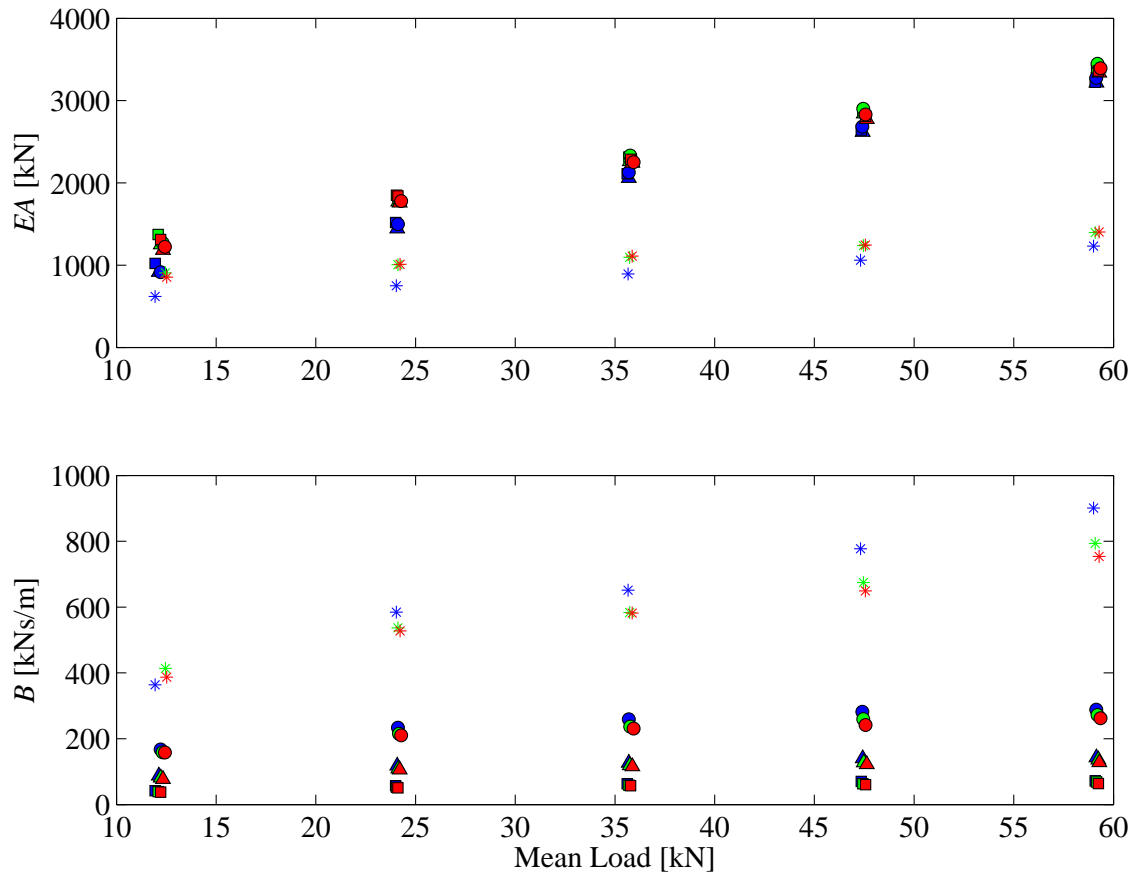


Fig. 6. Average (*top*) axial stiffness and (*bottom*) damping values for Sample 1 (blue markers), Sample 2 (green markers) and Sample 3 (red markers). Results are shown for oscillation periods, 100s (○), 50s (△) and 25s (□) as well as the initial creep/recovery load cycle (*).

and rearrangement of the rope construction (permanent or temporary) is suggested by the positive strain levels measured between each loading interval. Between each loading interval there was insufficient time for significant strain recovery to occur, and notable recovery was recorded after almost 11

hours of steady loading. The calculated strains reach a steady level after this time (on average 5.85%, Figure 5) with a similar magnitude to the final recovery cycles during bedding-in. Despite the different levels of strain obtained, especially during the bedding-in cycles, the range of final strain values

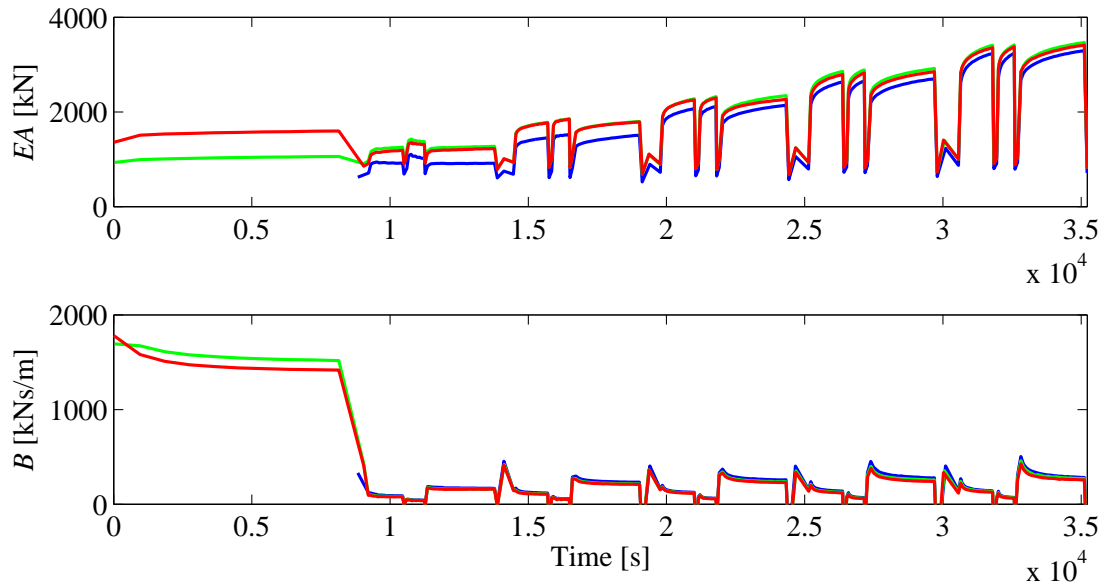


Fig. 7. Cycle-by-cycle calculated (*top*) axial stiffness and (*bottom*) damping for Sample 1 (blue line), Sample 2 (green line) and Sample 3 (red line). Negative damping values which correspond to extension-load loops which include significant sample recovery between harmonic intervals are not shown.

is small for the three samples, between 5.51-6.28%.

B. Axial stiffness and damping performance

1) *Influence of load rate:* Previous tests conducted by the authors on a section of aged rope of the same construction demonstrated that there was a dependency of harmonic oscillation period (and hence load rate) on both average axial stiffness and damping [20]. Based on the different ramp load rates used during bedding-in for the new rope samples (2 and 3) the axial stiffness values calculated are in agreement with this, in that the lower axial stiffness values correspond to bedding-in cycles with lower load rates. As with the previous study, the same inverse relationship between harmonic damping and load rate also exists for the new rope samples (Figure 6). However, unlike the previous study, the trend between load rate and axial stiffness is non-monotonic for the harmonic loading intervals. Whilst the same load levels were applied, the previous study differed in two respects: 1) a larger range of decreasing oscillation periods were used (100, 50, 25, 9, 6 and 3s), and 2) each interval was conducted as a separate test, allowing recovery to occur for several minutes between each harmonic interval. Results from the current study suggest that for the range of oscillation periods studied, the influence of load rate on axial stiffness is small. Instead, it is more likely that the evolution of strain (as shown in Figure 5) has a much greater influence, itself dependent on conditioning achieved during bedding-in.

2) *Influence of mean load level:* It was also shown in the previous study [20] that higher mean load levels resulted in steeper hysteresis loops, leading to higher average axial

stiffness and damping values. The same effect is demonstrated with the samples subjected to bedding-in (2 and 3) compared to Sample 1 (Figure 6). It is interesting to note that axial stiffness values calculated for the lower bedding-in level are marginally greater than those for the higher bedding-in level during harmonic loading. Whilst this contrasts the stiffness values calculated for the bedding-in cycles, this difference is small (up to 5.3%) for each load level and oscillation period. This effect may be explained by the difference in steepness of the unloading curves between 0-93.2kN during bedding-in (Figure 8). The calculated axial stiffness and damping values are scattered for the individual creep/recovery cycles, but there is a general increase of both quantities with increasing mean load.

Analysis of the measurement data on a cycle-to-cycle basis reveals that the axial stiffness of rope samples 2 and 3 reaches a fairly steady state during the bedding-in cycles. The application of progressively higher mean loads leads to a continued increase in axial stiffness during each harmonic interval. Both axial stiffness and damping start to become steady after 25 cycles (Figure 7) and it is expected that steady-state behaviour would be achieved after further load cycling. The evolution of both quantities with respect to energy transfer mechanisms will be the subject of a forthcoming publication. Due to time constraints, it was not possible to use more than 25 cycles for each harmonic loading interval. Whilst the application of many harmonic load cycles (of the order of several hundred or thousand) is a standard approach to determine the fatigue properties of

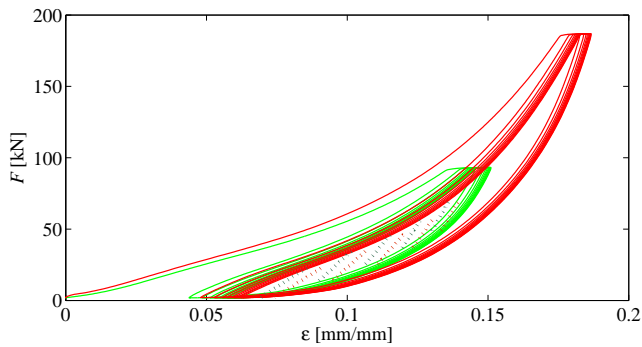


Fig. 8. Bedding-in hysteresis loops for Samples 2 (green line) and 3 (red line). Fitted single degree-of-freedom trend lines for the last cycle of each 100s harmonic interval are also shown (dashed lines)

synthetic ropes (e.g. [1]), the suitability of this approach is questionable for dynamically responsive buoy-like equipment, (i.e. MRE devices and the SWMTF) which are subjected to highly variable, non-harmonic loading regimes.

IV. CONCLUSION

In this study time-averaged and time-varying properties have been quantified for three parallel-stranded Nylon 6 mooring ropes subjected to mean loads and load rates that a buoy-like MRE device may experience in-service. By utilising different levels of bedding-in prior to applying a common loading profile to each sample (comprising a mixture of creep/recovery, harmonic and steady load intervals), the influence of load history on rope conditioning and properties has been investigated. The results presented in this study indicate that the use of bedding-in cycles has a significant influence on the performance of the rope due to the different levels of strain achieved prior to harmonic loading. The choice of bedding-in level specified for Nylon mooring lines prior to installation of a MRE device will therefore influence the short-term performance of the mooring system. The incorrect specification of bedding-in level may necessitate re-tensioning of the mooring lines if not achieved through environmental loading in the long-term. The axial stiffness and damping of the rope samples studied are both dependent on the mean load level applied. Whilst there is an inverse relationship between hysteresis damping and harmonic oscillation period, the trend between sample stiffness and harmonic oscillation period is non-monotonic. Calculation of these quantities on a cycle-to-cycle basis demonstrates that the previous load history will directly affect the instantaneous stiffness and damping of the line due to the level of strain achieved by the sample. In a forthcoming publication the energy transfer mechanisms associated with the evolution of rope characteristics will be presented, including a comparison between new and aged rope sample performance when subject to irregular loading regimes.

ACKNOWLEDGMENT

The authors would like to acknowledge the support of the MERiFIC project partners. The project is funded by the European Regional Development Fund through the Interreg IV-A programme.

REFERENCES

- [1] Bureau Veritas, "Certification of fibre ropes for deepwater offshore services. 2nd edition. ni 432 dto r01e," 2007.
- [2] International Standards Organisation, "Fibre ropes for offshore station keeping - polyester. ISO 18692," 2007.
- [3] Det Norske Veritas, "Offshore standard - position mooring. DNV-OS-E301," 2010.
- [4] American Bureau of Shipping, "Guidance notes on the application of fiber rope for offshore mooring," 2011.
- [5] I. Ridge, S. Banfield, and J. Mackay, "Nylon fibre rope moorings for wave energy converters," in *Proceedings of the OCEANS 2010 conference*, Seattle, USA, 2010.
- [6] The Carbon Trust, "Guidelines on design and operation of wave energy converters," 2005.
- [7] L. Johanning, G. Smith, and J. Wolfram, "Mooring design approach for wave energy converter," *Journal of Eng. For the Maritime Env (JEME)*, pp. 159–174, 2006.
- [8] L. Johanning, G. Smith, and J. Wolfram, "Measurements of static and dynamic mooring line damping and their importance for floating WEC devices," *Ocean Engineering*, pp. 1918–1934, 2007.
- [9] J. Fitzgerald and L. Bergdahl, "Including moorings in the assessment of a generic offshore wave energy converter: A frequency domain approach," *Marine Structures*, pp. 23–46, 2008.
- [10] S. Banfield, T. Veravel, R. Snell, and R. Ahilan, "Fatigue curves for polyester moorings - a state-of-the-art review," in *Proceedings of the 2000 Offshore Technology Conference (OTC 12175)*, Houston, USA, 2000.
- [11] H. da Costas Mattos and F. Chimisso, "Modelling creep tests in hmpe fibres used in ultra-deep-sea mooring ropes," *International Journal of Solids and Structures*, no. 1, pp. 144–152, 2011.
- [12] P. Davies, Y. Reaud, L. Dussud, and P. Woerther, "Mechanical behaviour of hmpe and aramid fibre ropes for deep sea handling operations," *Ocean Engineering*, pp. 2208–2214, 2011.
- [13] M. François, P. Davies, F. Grosjean, and F. Legerstee, "Modelling of fibre rope load-elongation properties - polyester and other fibres," in *Proceedings of the 2010 Offshore Technology Conference (OTC 20846)*, Houston, USA, 2010.
- [14] S. Weller, P. Davies, P. Thies, V. Harnois, and L. Johanning, "Durability of synthetic mooring lines for ocean energy devices," in *Proceedings of the 4th International Conference on Ocean Energy*, Dublin, Ireland, 2012.
- [15] P. Thies, L. Johanning, and G. Smith, "Towards component reliability testing for marine energy converters," *Ocean Engineering*, pp. 1918–1934, 2011.
- [16] International Electrotechnical Commission, "Marine energy - wave, tidal and other water current converters - part 10: The assessment of mooring system for marine energy converters. IEC-TS 62600-10 Ed.1.0 (in-progress)," 2012.
- [17] L. Johanning, P. Thies, and G. Smith, "Component test facilities for marine renewable energy converters," in *Marine Renewable and Offshore Wind Energy Conference*, London, UK, 2010.
- [18] J. Flory, S. Banfield, and D. Petruska, "Defining , measuring , and calculating the properties of fiber rope deepwater mooring lines," in *Proceedings of the Offshore Technology Conference (OTC 16151)*, Houston, USA, 2004.
- [19] J. Flory, C. Leech, S. Banfield, and D. Petruska, "Computer model to predict long-term performance of fiber rope mooring lines," in *Proceedings of the 2005 Offshore Technology Conference (OTC 17592)*, Houston, USA, 2005.
- [20] P. Thies, L. Johanning, T. Gordelier, V. A., and S. Weller, "Physical component testing to simulate dynamic marine load conditions," in *Proceedings of the 32nd International Conference on Ocean, Offshore and Arctic Engineering*, Nantes, France, 2013.